

Image based registration between full X-ray and spot mammograms for X-ray guided stereotactic breast biopsy

S. Said^a, P. Clauser^b, N.V. Ruiter^a, P.A.T. Baltzer^b, and T. Hopp^a

^aKarlsruhe Institute of Technology (KIT), Institute for Data Processing and Electronics,
Karlsruhe, Germany

^bMedical University of Vienna, Department of Biomedical Imaging and Image-guided Therapy,
Vienna, Austria

ABSTRACT

Breast cancer is the most dominant cancer type among women. Although digital mammography plays an important role in early breast cancer detection, many cancers cannot be distinguished on mammography only, particularly in individuals with dense breast tissue. Lesions not recognizable on mammography are frequently detected by contrast enhanced magnetic resonance imaging (CE-MRI) of the breast. Based on the suspicious characteristics, these lesions need to be further evaluated with MRI-guided biopsy. However, MRI-guided biopsy is costly, time consuming, and not commonly available. In our earlier work, we proposed a novel method for a matching tool between MRI and spot mammograms using a biomechanical model based registration to match MRI and full X-ray mammograms and an image based registration to align full X-ray mammograms and spot mammograms. In this paper, we focus on developing and evaluating methods for image based registration between full X-ray mammograms and spot mammograms. Results assessed for thirteen patients from the Medical University of Vienna are presented. The median target registration error (TRE) of the image based registration is 21.7 mm and the standard deviation is 9.3 mm.

Keywords: Image Based Registration, Image Similarity Metrics, Full Mammograms, Spot Mammograms

1. INTRODUCTION

For early diagnosis of breast cancer, medical imaging with different modalities has been used frequently to help doctors in qualitative diagnosis. Lesions, which are not visible when using traditional imaging methods such as X-ray mammography or ultrasound, could be detected by MRI.¹ However, detected lesions by MRI can be problematic in the clinical management of breast disease. As malignancy is found in approximately every second to third of such lesions, further workup is necessary.¹ These lesions may be either followed up or a biopsy is required based on the degree of suspicion.² While ultrasound can be used to identify and biopsy the suspicious lesion identified by MRI, a recent meta-analysis made by the team of Medical University of Vienna showed a limitation of ultrasound which has a probability for non detected lesions leading to cancer in up to 54% of the cases.³ In these specific cases, an MRI-guided biopsy is essential.³ MRI-guided biopsies, however, are costly and a recent survey showed a significant shortage of MRI-guided breast interventions world wide.⁴ A lack of MRI-guided breast interventions is a major limitation for a wider introduction of CE-MRI in clinical practice.⁵ A new approach for a clinical workflow has been proposed in our earlier work,⁶ which would allow to transfer lesions visible in MRI to spot mammograms and thereby enables cheaper and widely available X-ray guided biopsy. It consists of two methods: biomechanical model based registration between MRI and full X-ray mammograms^{7,8} followed by image based registration between full X-ray and spot mammograms. The biomechanical model based registration originates from our earlier work.⁹ The lesion detected by MRI is aligned with the full X-ray mammogram and it has been applied in an automatic registration workflow and tested with clinical datasets^{7,8}. An image based registration has been proposed to transfer the lesion position further from the full mammogram to the spot mammogram, which is taken during X-ray guided biopsy.⁶

In this paper, we focus on extension and deeper analysis of the second part: aligning the full mammograms with spot mammograms using an image based registration. We discuss different methods for image based registration. We test these methods using clinical datasets. We apply our methods to images from an X-ray guided biopsy device from Fischer Imaging Corp. in which the patient lies in a prone position.¹⁰

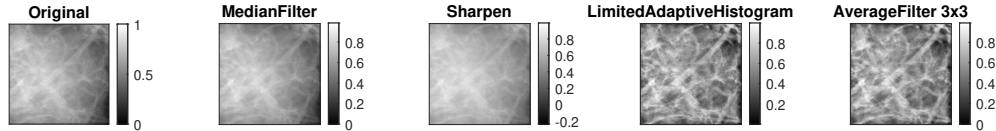


Figure 1. Process of enhancing spot mammograms in the fourth block of preprocessing.

2. METHODS

The general idea of this work is developing the methods to register full X-ray and spot mammograms using an image based registration. Each modality has a different imaging setup. For full mammograms, a 2D image of the patient in the upright standing position is acquired, while the breast is compressed up to 50% between two parallel compression plates. Full X-ray mammograms provide images with a pixel size less than 0.1 mm. There are two views usually taken in clinical routine: cranio-caudal (CC) mammograms are taken at a rotation angle of the X-ray tube and detector of 0° and mediolateral oblique (MLO) with angle 45° or -45° based on which side of the patient is imaged. For spot mammograms, a 2D image of size 50×50 mm with a detailed view of the compressed breast is taken in prone position in devices of e.g. Fischer and Lorad. In our setup we are using a Image Corporation device where spot mammograms provide images with a pixel size of 0.0488 mm. There are usually three views for taking a biopsy: CC, mediolateral (ML), and lateromedial (LM) with angle 0° , 90° , and -90° , respectively.

The proposed method consists of three steps: preprocessing, finding a region of interest (ROI) from the full mammogram, and then applying different image similarity metrics between the ROI and the spot mammogram while sliding the spot mammogram step by step over the ROI. This matching process allows resolving a translational transformation between both images. For CC views, we take into consideration that the spot mammogram at 0° rotation angle is in the same position as the full mammogram. For MLO views, we disregard the difference of rotation angle between full X-ray mammogram taken at MLO position and spot mammograms taken at ML or LM position. Hence, we assume that, the deformation state is comparable. The position of the maximum of the different image similarity is considered as the transformation parameter.

2.1 Preprocessing

For preprocessing, a resampling is applied first since spot mammograms have a resolution which may differ from the resolution of the full mammogram.¹⁰ Second, the spot mammogram is rotated by either 90° or 270° depending, on which breast was examined, in order to match the presentation of the breast in the full mammogram. Third, the spot mammogram's contrast is adapted to match the full mammogram. A normalization is done for both images and the intensities are converted to 255 intensity levels. Fourth, the image contrast is enhanced for both images by a method from Kumbhar, et al.¹¹ by first applying a median filter, followed by sharpening, equalization of the histogram and applying an average filter as shown in Figure 1. For speed up, the full mammogram is cropped to the nipple position in anteroposterior direction.

For MLO views in the full mammograms, only lesions inside the breast are currently considered, therefore we cut off the muscle in order to avoid aligning the spot mammogram with the muscle. First, we apply a sobel filter which is an edge detection filter followed by calculating the gradient magnitude of the image and then apply hough transform which is a feature extraction technique used in image analysis to detect the margin of the line that separates the muscle and the breast¹² as shown in Figure 2.

2.2 Region of Interest

In order to get the ROI from the full mammogram where the spot mammogram is potentially located, we propose a dynamic step size using a 2D convolution operation as a constraint for image similarity. We are measuring the convolution between small squares of size 50×50 mm from full mammogram and the spot mammogram. The dynamic step size depends on three factors. First, we get these squares from the full mammogram taking into consideration to cover the full mammogram iteratively. We are selecting these squares by calculating the

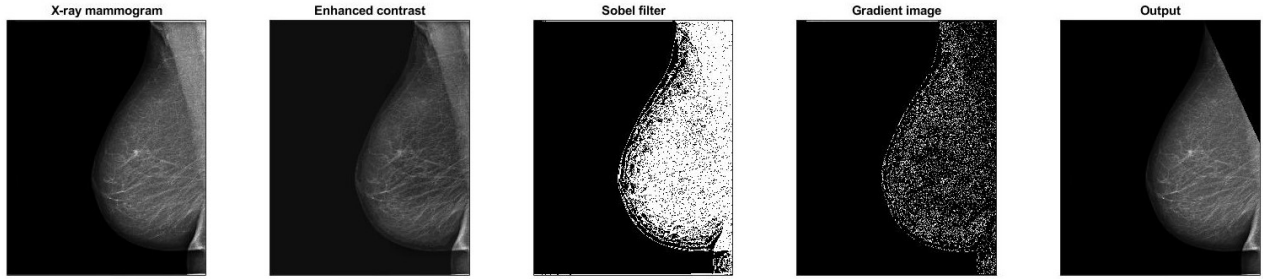
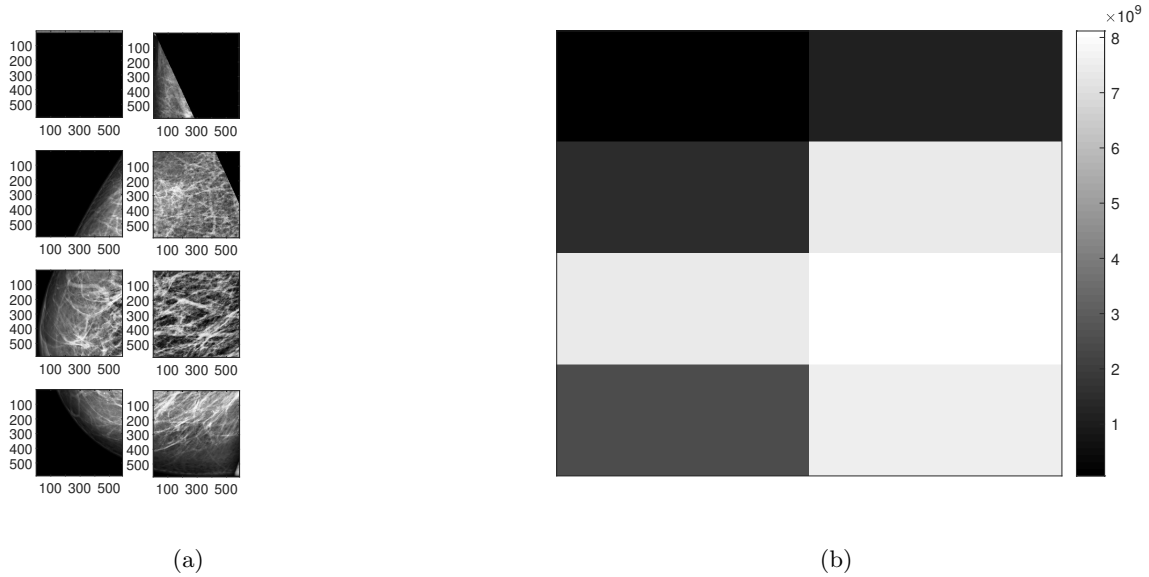


Figure 2. Process of removing muscle from the MLO views of the full X-ray mammograms.



(a)

(b)

Figure 3. The number of regions of the X-ray mammogram that are splitted in X and Y are two and four, respectively in the first iteration (a). The convolution values of the eight regions shows that the higher the value, the higher the probability of the ROI containing the spot mammogram is (b).

ratio between X and Y coordinates of the input of X-ray mammograms and we split the X coordinate into a specific number of parts in each iteration. Based on the ratio and these partitions of X, partitions of Y will be calculated. Second, we calculate the histogram of convolution values in all squares for all iterations and we look in each iteration for the last bin width and check how many areas in this last bin width (the maximum convolution values) are. Third, after a defined number of iterations combined together, we crop the input of the full mammogram to the region with the maximum convolution values. Based on empirical tests on our available data, we are doing six iterations, splitting X coordinate in two, four, six, four, eight, and twelve parts, respectively in each iteration, and we are cropping once at the third iteration and once at the sixth iteration as shown in Figure 4.

It is illustrated for example in the first iteration as shown in Figure 3. We are splitting X coordinate in two parts. Based on that and the ratio of X related to Y is two. Hence, Y coordinates are splitted into four parts. We apply the convolution operation for these eight regions with the spot mammograms. We get the areas that has the maximum of the convolution values, i.e. the bright areas in Figure 3 (b), which is four areas in this case. The higher the value, the higher the probability of the ROI containing the spot mammogram is.

2.3 Image Similarity

After getting the ROI from the full mammogram as shown in Figure 4 (c), we apply a rescaling factor of 0.1 for computational speed up for both ROI and spot mammogram images. The spot mammogram is slid across the ROI pixel by pixel. At each position we calculate the image similarity between the spot mammogram and the underlying area in the full mammogram (ROI). In this paper we consider several image similarity metrics in order to evaluate which one works best.

The first class of quality measures is Partitioned Intensity Uniformity (PIU) and Ratio Image Uniformity (RIU). PIU is based on partitioning the pixels in one image into iso-intensity based on the histogram bins and then the sum of the normalized standard deviation of the corresponding pixels for each iso-intensity set in the other image is computed.¹³ RIU is a variant of PIU using the division of the two images pixel by pixel and then getting a ratio between the standard deviation and mean. The second class of quality measures is mutual information (MI) and normalized mutual information (NMI). Both of them are based on the definitions of the entropy, joint histogram, and joint entropy between two images^{14, 15}

The third class of quality measures is measuring the correlation coefficient which is the difference between the intensity value at that pixel and the mean intensity of the whole image for every pixel location in both images. The fourth class is a 2D convolution, performing an element-wise multiplication and then summing up results into a single output pixel. The fifth class of quality measures Mean Square Error (MSE), Signal to Noise Ratio (SNR), and Peak Signal to Noise Ratio (PSNR). MSE and SNR is measuring the mean square error and the signal to noise ratio between the two images. For PSNR, we take the peak signal to noise ratio of the moving image referenced to the spot mammogram.

2.4 Evaluation Method

We use annotated lesions in the two modalities as a benchmark to assess the accuracy of our registration algorithms. The Euclidean distance between the center of the predicted lesion in the registered image and the center of the annotated lesion from the radiologist in the unregistered image is defined as the Target Registration Error (TRE).

3. RESULTS

We tested the method using thirteen patient datasets from the Medical University of Vienna. The datasets of full X-ray mammograms consisted of five full field digital CC (left and right) and eight MLO (left and right) mammogram views. Twelve patients are taken from Siemens Mammomat Inspiration and one patient is taken from Philips Mammo MicroDose L30 digital mammography device. Spot view mammograms are taken during X-ray guided biopsy on a Fischer table. The datasets of spot mammograms consisted of five CC views (left and right), seven of ML views (left and right), and one of LM view (left). As a landmark for assessing the registration quality, four points representing the maximal expansion of a lesion in each direction in both full and spot mammogram were acquired from a radiologist. The center point was calculated as the arithmetic mean of these points.

From the analysis as shown in Figure 5 (a), MSE is considered the most robust image similarity metric for the particular problem. The median TRE of thirteen patients is 21.7 mm. The lower and the upper quarter are 20.2 and 29.5 mm, respectively while the minimum and the maximum values are 3.4 mm and 37.9 mm, respectively. In RIU, PSNR, and SNR, the lower and the upper quarter varies from 32 till 38.4 mm and from 70 till 89.5 mm, respectively. While using the correlation similarity metric, the lower and the upper quarter are 11.7 mm and 80 mm. Those four metrics are the worst and considered to be left out from the comparison. However, for MI, NMI, PIU, and convolution, the lower and the upper quarter varies from 7 till 19.4 mm and from 40 till 48 mm, respectively. Even though the differences in rotation angles for MLO and ML views in full X-ray mammograms and spot mammograms, respectively has not been considered, the method shows promising results. We divided the results into two subgroups CC/MLO views as shown in Figure 5 (b). It shows that median of TRE is decreasing in CC in some image similarity metrics such as NMI and MI. While for the median of MSE, which is the most robust one, is nearly the same in MLO and CC views.

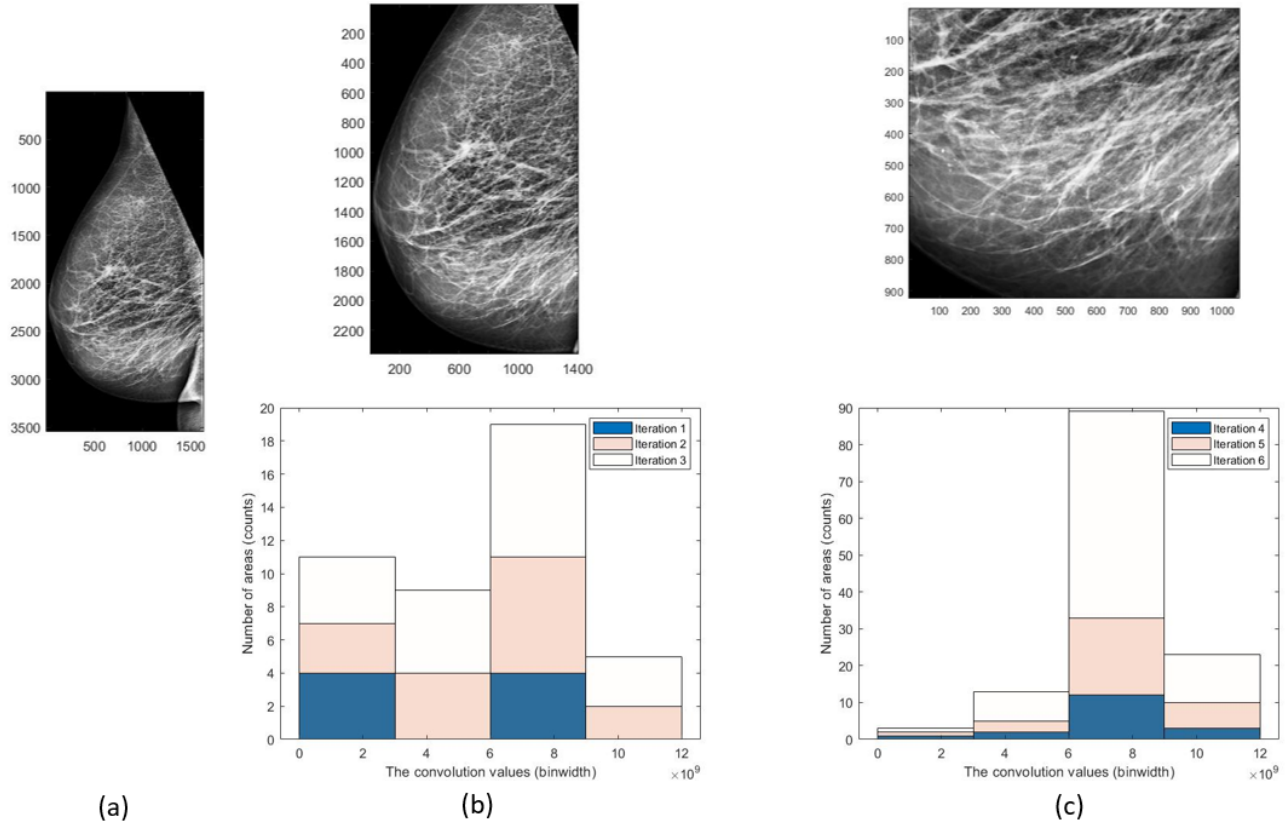


Figure 4. Input for the dynamic stepping process to find the ROI (a). The ROI from the full mammogram after three iterations from the dynamic stepping process (top) and showing the histogram of the convolution operation in the first, second, and third iterations (bottom) (b). The ROI from the full mammogram after six iterations from the dynamic stepping process (top) and showing the histogram of the convolution operation in the fourth, fifth, and sixth iterations (bottom) (c).

An example for the annotation is shown in Figure 6 (a). The green lesion represents the lesion that is marked by the radiologist and the blue lesion represents the predicted lesion based on the annotation in the spot mammogram. An example for the annotation of the two steps together using biomechanical and image based registration is shown in Figure 6 (b). The blue lesion represents the lesion that is marked by the radiologist and the red lesion represents the predicted lesion based on the two steps together. The TRE of our image based registration is 21.4 mm while The TRE of our biomechanical based registration is 22.7 mm. The total TRE of two steps together is 5.2 mm.

4. DISCUSSION AND CONCLUSION

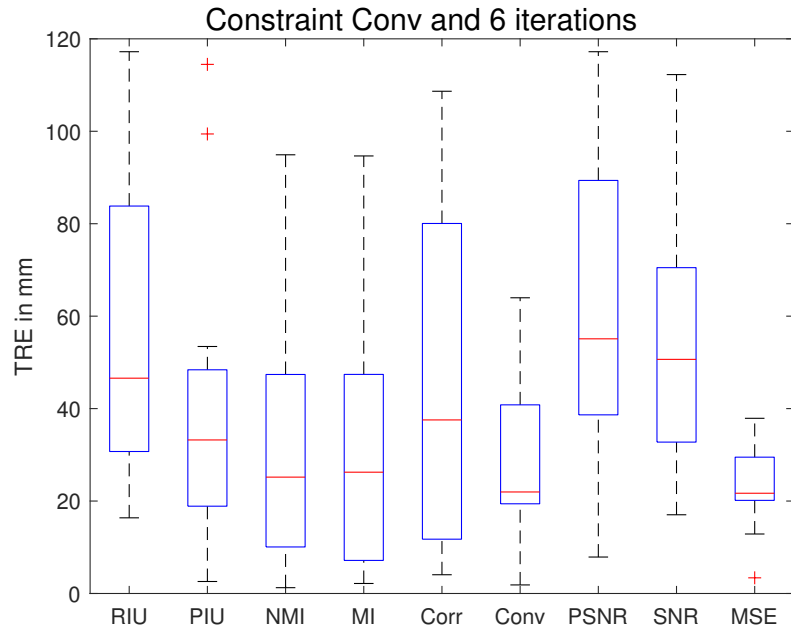
To our best knowledge, an image based registration between full X-ray and spot mammograms for X-ray guided stereotactic breast biopsy has not been presented before. Our proposed methods provide encouraging results with a median TRE of 21.7 mm. While the median error is already relevant for clinical application, more research for potential improvements of the case, e.g. with the large error of 37.9 mm is required. We suspect that more optimal parameters such as the number of iterations or restricting the search of the ROI to anatomically plausible regions may improve such outliers. In the future, we would like also to validate the results with more clinical datasets. Also, we would like to consider the deformation state of the two images and the difference of rotation angles using affine transformation and not only translational transformation. Our presented method here in combination with the earlier presented registration workflow will provide the ability to use X-ray guided biopsy instead MRI-guided interventions.

ACKNOWLEDGMENTS

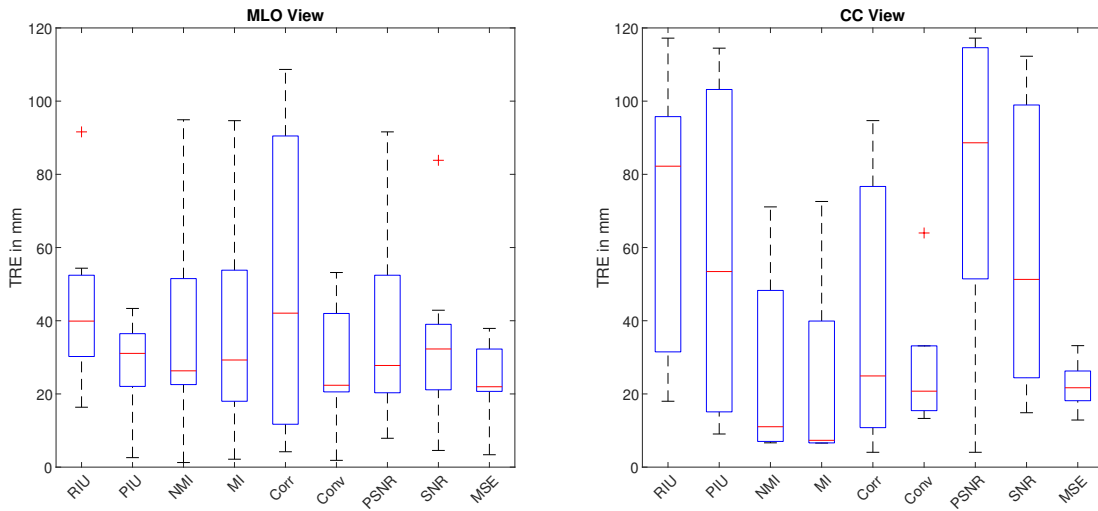
This work was funded by the German Research Foundation (DFG) under grant number 5565/3-1 and the Austrian Science Fund (FWF) under grant number 4240.

REFERENCES

- [1] Houssami, N., Ciatto, S., Macaskill, P., Lord, S. J., Warren, R. M., Dixon, J. M., and Irwig, L., “Accuracy and Surgical Impact of Magnetic Resonance Imaging in Breast Cancer Staging: Systematic Review and Meta-Analysis in Detection of Multifocal and Multicentric Cancer,” *Journal of Clinical Oncology* **26**(19), 3248–3258 (2008).
- [2] Mann, R., Balleyguier, C., Baltzer, P., Bick, U., Colin, C., Cornford, E., Evans, A., Fallenberg, E., Forrai, G., Fuchsjäger, M., Gilbert, F., Helbich, T., Heywang-Köbrunner, S., Herrero, J., Kuhl, C., Martincich, L., Pediconi, F., Panizza, P., Pina, L., and Sardanelli, F., “Breast MRI: Eusobi recommendations for women’s information,” *European Radiology* **25** (05 2015).
- [3] Spick, C. and Baltzer, P. A. T., “Diagnostic utility of second-look US for breast lesions identified at MR imaging: Systematic review and meta-analysis,” *Radiology* **273**(2), 401–409 (2014). PMID: 25119022.
- [4] Clauser, P., Mann, R., Athanasiou, A., Prosch, H., Pinker, K., Dietzel, M., Helbich, T. H., Fuchsjäger, M., Camps-Herrero, J., Sardanelli, F., Forrai, G., and Baltzer, P. A. T., “A survey by the European Society of Breast Imaging on the utilisation of breast MRI in clinical practice,” *European Radiology* **28**, 1909–1918 (May 2018).
- [5] Kuhl, C. K., Strobel, K., Bieling, H., Wardelmann, E., Kuhn, W., Maass, N., and Schrading, S., “Impact of preoperative breast MR imaging and MR-guided surgery on diagnosis and surgical outcome of women with invasive breast cancer with and without DCIS component,” *Radiology* **284**(3), 645–655 (2017).
- [6] Said, S., Clauser, P., Ruiter, N. V., Baltzer, P. A. T., and Hopp, T., “Image registration between MRI and spot mammograms for X-ray guided stereotactic breast biopsy: preliminary results,” in [*Medical Imaging 2021: Image-Guided Procedures, Robotic Interventions, and Modeling*], Linte, C. A. and Siewerdsen, J. H., eds., **11598**, 354 – 361, International Society for Optics and Photonics, SPIE (2021).
- [7] Hopp, T., Baltzer, P., Dietzel, M., Kaiser, W., and Ruiter, N., “2D/3D image fusion of X-ray mammograms with breast MRI: Visualizing dynamic contrast enhancement in mammograms,” *International Journal of Computer Assisted Radiology and Surgery* **7**, 339–48 (06 2011).
- [8] Hopp, T., Dietzel, M., Baltzer, P., Kreisel, P., Kaiser, W., Gemmeke, H., and Ruiter, N., “Automatic multi-modal 2D/3D breast image registration using biomechanical FEM models and intensity-based optimization,” *Medical Image Analysis* **17**(2), 209–218 (2013).
- [9] Ruiter, N. V., Stotzka, R., Müller, T., Gemmeke, H., Reichenbach, J. R., and Kaiser, W. A., “Model-based registration of X-ray mammograms and MR images of the female breast,” *IEEE Transactions on Nuclear Science* **53**(1), 204–211 (2006).
- [10] Carr, J. J., Hemler, P. F., Halford, P. W., Freimanis, R. I., Choplin, R. H., and Chen, M. Y. M., “Stereotactic Localization of Breast Lesions: How It Works and Methods to Improve Accuracy,” *RadioGraphics* **21**(2), 463–473 (2001). PMID: 11259709.
- [11] Kumbhar, U. S., Patil, V., and Rudrakshi, S., “Enhancement of Medical Images Using Image Processing in Matlab,” *International Journal of Engineering Research and Technology* **2** (2013).
- [12] Bora, V. B., Kothari, A. G., and Keskar, A. G., “Robust automatic pectoral muscle segmentation from mammograms using texture gradient and euclidean distance regression,” *Journal of Digital Imaging* **29**, 115–125 (February 2016).
- [13] Wu, J., Kim, M., Peters, J., Chung, H., and Samant, S. S., “Evaluation of similarity measures for use in the intensity-based rigid 2D-3D registration for patient positioning in radiotherapy,” *Medical Physics* **36**(12), 5391–5403 (2009).
- [14] Maes, F., Collignon, A., Vandermeulen, D., Marchal, G., and Suetens, P., “Multimodality Image Registration by Maximization of Mutual Information,” *IEEE Transactions on Medical Imaging* **16**(2), 187–198 (1997).
- [15] Studholme, C., Hill, D., and Hawkes, D., “An overlap invariant entropy measure of 3D medical image alignment,” *Pattern Recognition* **32**(1), 71–86 (1999).



(a)



(b)

Figure 5. Image similarity metrics of thirteen patients in MLO/CC views and left/right breast for full X-ray mammograms and ML/LM/CC views and left/right breast for spot mammograms for image based registration based on dynamic step size with convolution constraint (6 iterations). All of the datasets were rescaled for processing with a factor 0.1 after applying the dynamic stepping to determine the ROI in (a). The subgroups of both views MLO/CC for the thirteen patients (b).

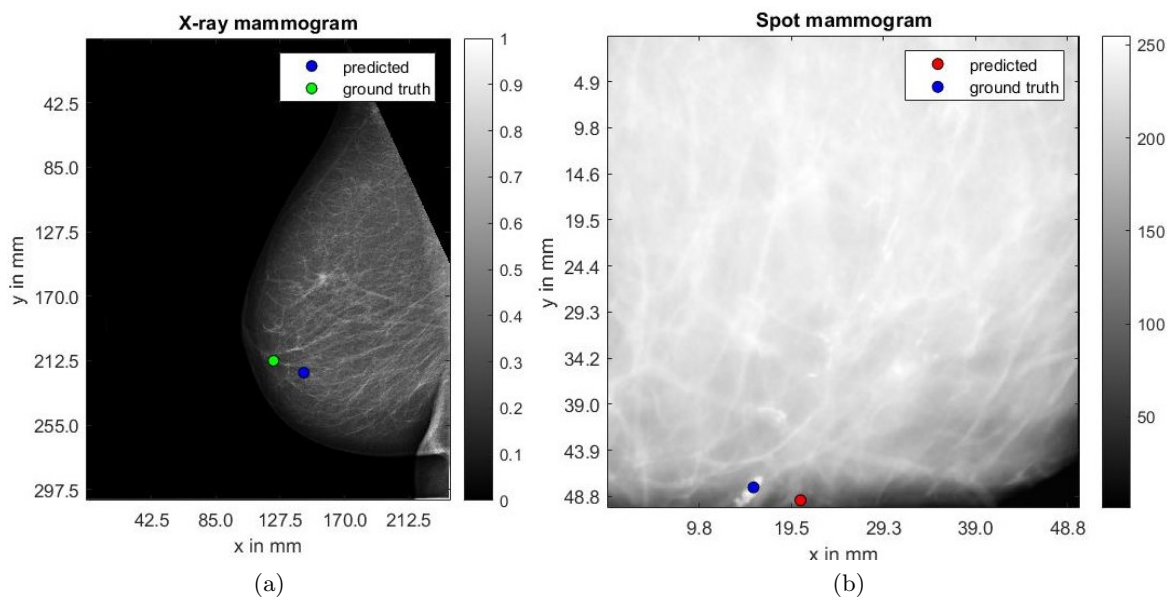


Figure 6. Example of the predicted lesion (blue) in one of the cases in the full mammogram using image based registration (a). Example of the predicted lesion (red) in the same case in the spot mammogram using the two methods together: biomechanical based registration and image based registration (b).